Calibrating soybean parameters in JULES 5.0 from the US-Ne2/3 FLUXNET sites and the SoyFACE-O₃ experiment

Felix Leung[1,3], Karina Williams[2,7], Stephen Sitch[1], Amos P.K. Tai[3,6], Andy Wiltshire[2], Jemma Gornall[2], Elizabeth A. Ainsworth[4], Timothy Arkebauer[5], David Scoby [5]

5   [1] College of Life and Environmental Sciences, University of Exeter, Exeter, EX4 4RJ, UK.

[2]Met Office Hadley Centre, FitzRoy Road, Exeter, Devon, United Kingdom

[3]Earth System Science Programme, Faculty of Science, and Institute of Environment, Energy and Sustainability, The Chinese University of Hong Kong, Hong Kong

[4]USDA ARS, Global Change and Photosynthesis Research Unit, Urbana, Illinois, USA

10   [5] Department of Agronomy and Horticulture, University of Nebraska-Lincoln, Lincoln, Nebraska, USA

[6] State Key Laboratory of Agrobiotechnology, The Chinese University of Hong Kong, Hong Kong

[7]Global System Institute, University of Exeter, Laver Building, North Park Road, Exeter EX4 4QE, UK

Correspondence to: Felix Leung (felix.leung@cuhk.edu.hk)

Abstract. Tropospheric ozone (O_3) is the third most important anthropogenic greenhouse gas. O_3 is detrimental
15   to plant productivity, and it has a significant impact on crop yield. Currently, the Joint UK Land Environment Simulator (JULES) land surface model includes a representation of global crops (JULES-crop), but does not have crop-specific O_3 damage parameters, and applies default C3 grass O_3 parameters for soybean that underestimates O_3 damage. Physiological parameters for O_3 damage in soybean in JULES-crop were calibrated against leaf gas-exchange measurements from the Soybean Free-Air-Concentration-Enrichment (SoyFACE) with O_3 experiment
20   in Illinois, USA. Other plant parameters were calibrated using an extensive array of soybean observations such as crop height, leaf carbon, etc. and meteorological data from FLUXNET sites near Mead, Nebraska, USA. The yield, aboveground carbon and leaf area index (LAI) of soybean from the SoyFACE experiment were used to evaluate the newly calibrated parameters. The result shows good performance for yield, with the modelled yield being within the spread of the SoyFACE observations. Although JULES-crop is able to reproduce observed LAI
25   seasonality, its magnitude is underestimated. The newly calibrated version of JULES will be applied regionally and globally in future JULES simulations. This study helps to build a state-of-the-art impact assessment model and contribute to a more complete understanding of the impacts of climate change on food production.

1 Introduction

Surface ozone (O_3) pollution is one of the major threats to global food security due to the detrimental effects of ozone exposure on crops (Ainsworth et al., 2012; Avnery et al., 2011b; Leung et al., 2020; Long et al., 2005; Tai et al., 2014; Tai andVal Martin, 2017). In the United States alone, crop loss due to tropospheric O_3 costs more than \$5 billion USD annually (Ainsworth et al., 2012; Avnery et al., 2011a; Van Dingenen et al., 2009).

Soybean is one of the main staple crops for human consumption; it also serves as an important source of animal feed. It is a cheap source of proteins and therefore soybean products are consumed around the world. The impact of O_3 on soybean physiology and growth has been studied extensively (Ainsworth et al., 2012; Betzelberger et al., 2012; Dermody et al., 2008; Morgan et al., 2003). Crop yield losses to tropospheric O_3 have been quantified using model projection and experiments. The National Crop Loss Assessment Network and European Open Top Chamber programs have established the air quality guideline, which derived dose-response relationships from comparable experimental data. These campaigns provided critical information such as the O_3 response relationship and estimated yield loss due to O_3 damage that enabled regional projections of O_3 effects on crop yields (Fuhrer, 2009). However, open top chambers modify plant response to O_3 due to the 'chamber effects' which create microclimates (Elagöz and Manning, 2005) and environmental differences between the chamber and open air micrometeorology in which yield loss is underestimated (Van Dingenen et al., 2009). Recently the introduction of Free-Air-Concentration-Enrichment (FACE) technology avoids the artefacts from enclosed chambers, and O_3 fumigation was adapted to FACE facilities (Agathokleous et al., 2017; Paoletti et al., 2017). The application of FACE experiment on crops took place in China (Zhu et al., 2011) and USA, including experiments with soybean at the SoyFACE experiment in Champaign, Illinois (Morgan et al., 2004; Betzelberger et al. 2010; 2012).

Crops are a significant component of the land surface; e.g., croplands and pasturelands represent 12% and 26% of the global terrestrial land, respectively (Van den Hoof et al., 2011). Moreover, the phenology of crops is very different from that of natural vegetation, and is characterized by high growth, turnover rate, and strong seasonality. It is thus necessary to include a crop-specific parameterization scheme to improve simulations of land surface fluxes and regional climate in agroecosystems (Van den Hoof et al., 2011). The Joint UK Land Environment Simulator with crops (JULES-crop) is a crop parameterisation (Osborne et al., 2015) within the land surface model, JULES (Best et al., 2011; Clark et al., 2011). Global simulations have been performed with

60   JULES-crop for rice, wheat, maize and soybean (Osborne et al., 2015). These four crop types contribute more than 70% of human calorie intake (Ray et al., 2013). JULES-crop includes routines representing growth, development and harvesting of crops driven by the overlying meteorological inputs. In JULES-crop, four new prognostic variables have been added: crop development index (DVI), root carbon (Croot), harvest carbon (Charv) and reserve carbon (Cresv). DVI controls the duration of the crop growing season in four distinct stages:

65   sowing, emergence, flowering, and maturity, and it determines when changes in carbon partitioning occur (Osborne and Hooker, 2011). Croot, Charv, and Cresv are the carbon pools for roots, harvested organs (e.g. grains of cereal, fruits, and root) and stem reserves, respectively. Carbon pools for stem and leaves are determined from the existing prognostic variables, LAI (Leaf area index) and canopy height. In Osborne et al. (2015), global runs of maize, wheat, soybean and rice were carried out using JULES-crop. Site runs were performed at four

70   FLUXNET sites with soybean-maize rotation: Bondville (US-Bo1), Fermi (US-IB1) and Mead (US-Ne2 and US-Ne3). Simulated yield was compared against country and global FAO crop yields. Osborne et al. (2015) used generic representations for each of the crops in their global study. For the plant parameters that are needed outside the crop model such as leaf nitrogen and leaf respiration parameters, these are set to those of the C3 or C4 grass functional types. Osborne et al. (2015) suggested that these parameters could be tuned to be more crop

75   specific to improve fit to observations. These JULES parameters have been calibrated against observations for maize, using data from the Mead FLUXNET sites in Nebraska (Williams et al., 2017). However, to date, these parameters have not been calibrated to soybean data.

       There are many crop models developed by institutions / organisations around the world. Most are designed for

80   application to an individual field up to the regional scale and do not include O_3 impacts on vegetation. (Supplementary Materials Table A1) compares a selection of land surface models which include crop tiles and have the functions to model climate impact on crop productivity. JULES-crop is of particular interest because it is a development of the global land surface component JULES of the Met Office numerical weather prediction and climate models, and contains a detailed representation of plant physiological processes at sub-

85   diurnal timescales, including consideration of O_3 effects on natural vegetation, thus making it suitable for this study. JULES-Crop has been accepted into the JULES trunk with the intention to be coupled with the Hadley Centre Global Environment Model (HadGEM) in the near future. HadGEM is recognised as one of the best performing climate models with smaller errors than typical climate models (Gleckler et al., 2008; Knutti et al., 2013).

90

The calibration of O_3 damage on soybean would allow land surface and crop models to more realistically and reliably simulate present-day and future O_3 damage, and subsequently to quantify its economic impacts. The objective of this study is to calibrate soybean representation for JULES-crop, with a particular focus on the response of soybean to O_3 exposure.

This paper is organised as follows: Section 2 describes the model set-up and observations used for the JULES calibration. Section 3 compares the results from the calibrated JULES runs against independent observations. Section 4 assesses the suitability of the model for modelling soybean under O_3 damage and discusses ways of future model improvement.

2 Methods

A flowchart demonstrating the calibration and evaluation procedure is given in Figure 1. We first tuned the JULES-crop soybean parameterisation at the US-Ne2 and US-Ne3 Mead sites, where three years of soybean physiological and meteorological observations were available, at ambient ozone (Figure 1, steps 1-5). The three years are 2004, 2006 and 2008 which soybeans were grown in Mead, maize were grown in other years.

Secondly, to calibrate the JULES ozone damage parameters (Figure 1, step 6) we made the assumption that there is a negligible damage to crop yield at ambient background levels of O_3 at both the SoyFACE and Mead sites. This is consistent with Mills et al. (2007), who reviewed over 700 published papers and conference proceedings and found that O_3 level of AOT40 over 3 months of 5 ppm-h reduced soybean yield by less than 5%. Then we calibrated specifically the soybean O_3 response using leaf gas exchange measurements from soybean grown under elevated O_3 concentrations at SoyFACE.

Finally, we applied JULES-crop newly calibrated for soybean and its O_3 sensitivity at the leaf-level and evaluated model performance against observed yield and leaf area index from SoyFACE, taken for the full range of rings and cultivars (Figure 1, step 7).

2.1 Calibration of soybean in the absence of ozone damage, using observations from Mead

We followed the standard tuning procedure performed on maize by Williams et al., (2017) but applied to soybean (Figure 1, steps1-5). Step 1 involves using Mead observation to tune the parameters needed by all PFTs in JULES with the crop model switched off. Step 2 is to evaluate the model performance of GPP using Mead meteorlogy and LAI. Step 3 tunes the parameters needed by crop only. Step 4 evaluates the JULES-crop run performance with observed carbon pools in leaf, stem, harvest etc. Step 5 demonstrates the full JULES-crop runs at Mead using Mead meteorlogy and compared the model with observed GPP, aboveground carbon etc. Step 6 tunes ozone damage using SoyFACE LiCOR measurements. And finally step 7 evaluates JULES-crop performance using SoyFACE meteorology and compare with observed yield and LAI. This method is described in detail in the Supplementary Material, and the resulting parameters are given in Table 1-3. These are compared to the parameters used in Osborne et al. (2015), which we refer to as the "Osborne 2015 tuning". Note that the parameters in Table 3 in the Osborne 2015 tuning are typical defaults for C3 grass, rather than soybean-specific.

2.2 Calibration of JULES ozone damage parameters

2.2.1 Ozone effects on vegetation (exposure-response)

Many studies have shown that the impacts of O_3 are closely related to accumulated exposure above a threshold concentration rather than the mean growing season concentration (Forestry Commission, 2016; Gerosa et al. 2012; Mills et al. 2007). An index of accumulated exposure above a threshold concentration of x ppb (AOTx) has thus been developed as a measure of assessing O_3 pollution effects on vegetation. AOTx is calculated as the summed product of the concentration above the threshold concentration and time (T), with values expressed in ppb h or ppm h. (Mills et al. 2007; Forestry Commission, 2016).

The O_3 exposure index AOT40: Accumulated O_3 exposure over a threshold of 40 parts per billion (Equation 1) has been widely used by crop impact models in the forestry and agriculture industry and was used at SoyFACE.

$$AOT40 = \int \max(O_3 - 40 ppb, 0.0)\, dt \qquad (1)$$

The metric ensures only O_3 concentrations above 40 ppb are included. The integral is taken over daytime hours between 0700 to 1900. AOT40 does not account for the actual uptake of O_3 by plants and how this varies with ontogenetic (life span of the plant) and climatic factors such as temperature, irradiance, vapour pressure deficit, and/or soil moisture (Ashmore, 2005; Fuhrer et al. 1997).

There is a drawback of the cumulative O_3 exposure indices (Pleijel et al. 2000), which assume an instantaneously fixed threshold flux below which there is no effect of O_3, which may not be realistic. Also in nature, the threshold value is unlikely to be constant (Ashmore, 2005) since the capacity of detoxification of O_3 varies with climate and plant species. To improve these indices, the Stockholm Environment Institute developed the Deposition of Ozone for Stomatal Exchange model (DO_3SE) (Emberson et al., 2007; ICP Vegetation, 2017). DO_3SE was developed to estimate the risk of O_3 damage to European vegetation and is capable of providing O_3 flux estimation by evaluating the soil water deficits and their influence on stomatal conductance which affect plant O_3 uptake. Phyto-toxic O_3 dose (POD) above a stomatal threshold over a growing season (the accumulated stomatal flux above threshold Y) PODy can differentiate species sensitivity to rising background concentration, while AOT40 can only incorporate the effect of rising global background O_3 above the threshold 40ppb. This difference means AOT40 metric is less sensitive to O_3 peaks, and stomatal flux based metric (e.g. PODy and DO3SE) perform better on O_3 damage estimation in general (Büker et al., 2012; Dentener, F., Keating, T., and Akimoto, 2010; Pleijel et al., 2007).

2.2.2 Description of ozone response scheme in JULES

The current O_3 scheme in JULES uses a dose-response approach to model O_3 damage (Sitch et al., 2007; Clark et al., 2011). It uses the O_3 concentration in the atmosphere to modify net photosynthesis A_p by an O_3 uptake factor $\boldsymbol{F}$:

$$A = A_p \boldsymbol{F} \quad (2)$$

where $\boldsymbol{F}$ represents the fractional reduction of plant production:

$$\boldsymbol{F} = 1 - aUO_{>FO3crit} \qquad (3)$$

It assumes that O_3 suppresses the potential net leaf photosynthesis in proportion to the O_3 flux through stomata above a specified critical threshold (Clark et al., 2011).

$UO_{>F\ O3crit}$ is the instantaneous leaf uptake of O_3 over a plant functional type specific threshold (F_{O3crit}) (nmol $m^{-2}s^{-1}$) and the plant type specific parameter a is the fractional reduction of photosynthesis with O_3 uptake by leaves (Clark et al., 2011; Sitch et al., 2007).

$$UO_{>FO3crit} = \max[(F_{O3} - F_{O3crit}), 0.0] \quad (4)$$

From equations 3 & 4, F depends on the O_3 uptake rate by stomata (F_{O3}) over a critical (plant functional type specific) threshold for damage. It uses an analogy of Ohm's law, the O_3 flux through stomata, F_{O3} (nmol O_3 m^{-2} s^{-1}), is given by,

$$F_{O3} = \frac{[O_3]}{R_a + \left[\frac{\kappa_{O3}}{g_l}\right]} \quad (5)$$

where $[O_3]$ is the molar concentration of O_3 at reference level (nmol m^{-3}), R_a is the combined aerodynamic and boundary layer resistance between leaf surface and reference level (s m^{-1}). g_l is the leaf conductance for H_2O (m s^{-1}), and $\kappa_{O3} = 1.67$ is the ratio of leaf resistance for O_3 to leaf resistance for water vapour [Sitch et al., 2007]. The uptake flux is dependent on the stomatal conductance, which is reliant on the photosynthetic rate in JULES. Given that g_l and photosynthetic rate are linearly related [Cox et al., 1999], g_l is given by,

$$g_l = g_p F \quad (6)$$

Where g_p is the leaf conductance in the absence of O_3 effects. The set of equations (3,5,6) produces a quadratic relationship as a function of F, that can be solved analytically (Sitch et al., 2007).

Fractional reduction of photosynthesis with the instantaneous uptake of O_3 by leaves (mmol m^{-2}) determines the sensitivity of soybean to O_3 and the PFT-specific O_3 critical level (FO$_3$ crit) determines the threshold O_3 flux above which would cause damage to photosynthesis (Oliver et al., 2018; Sitch et al., 2007). The higher the sensitivity of plants to O_3 the lower photosynthesis the plant has at a given constant critical threshold. Sitch et al. (2007) configured plant functional types with two different O_3 sensitivities (fractional reduction of photosynthesis by O_3, F, equation 2, 3), where $a = 1.40$ is high sensitivity, and $a = 0.25$ is lower sensitivity for C3 grass (Sitch, 2007), using monthly average O_3 data and calibration to yield observations.

2.2.3 Calibrating the ozone effects on crop leaf photosynthesis in JULES using SoyFACE

The SoyFACE experiment in Illinois allows controlled CO_2 or O_3 enrichment across large plots within a soybean field without an enclosure. SoyFACE O_3 fumigation typically began after the emergence of soybean, and the plots

were fumigated with O_3 for 8–9 hours daily except when leaves were wet. In 2009 and 2010, soybeans were exposed to nine different concentrations of O_3 ranging from the ambient level to a target level of 200 ppb (Supplement Figure A2). The fumigation ended when soybean was mature.

Plant damage from O_3 is cumulative and the target concentration for the experiment was not always met (e.g., when wind speeds are low, during rain or when O_3 generators or analyzers are down). Therefore, the 8-hour mean and the AOT40 index (Accumulated Ozone exposure above the Threshold of 40 ppb) were used for the analysis in SoyFACE instead of using the target O_3 concentration. The planting dates were June 6, 2009 (Day 159) and May 27, 2010 (Day 157). Fumigation began on June 29, 2009 (Day 179 - 260) and June 6, 2010 (Day 167 -271) and harvest occurred on October 20, 2009 (Day 293) and September 20, 2010 (Day 273). O_3 concentrations measured at SoyFACE fluctuated greatly, as they were strongly influenced by weather conditions, especially by wind speed. The magnitude of O_3 concentration fluctuations in the high targeted concentration was greater than the low concentration (Supplement Figure A2). On some days of the year when the fumigation was off, very low O_3 concentrations were recorded for all target rings.

To calibrate the O_3 parameters for soybean in JULES-crop, we used midday photosynthetic gas-exchange measurements from Betzelberger et al. (2012). These were taken at four stages during the growing season, from seven soybean cultivars growing at 9 different O_3 concentrations, using open gas exchange systems (LI-6400 and LI-6400-40). These observations were used in conjunction with the daytime 8-hour mean O_3 concentration measurements and the parameters calibrated at the Mead site to drive the Leaf Simulator computer package, which reproduces the calculation of leaf photosynthesis within JULES. We then tuned the O_3 parameterisation of Fractional reduction of photosynthesis by O_3 (sensitivity) and Threshold of O_3 flux (nmol m-2 s-1) to match the modelled leaf photosynthesis rate to the observed rate (Figure 2). The tuned parameters are showed in Table 4.

2.3 Model configuration for the JULES-crop SoyFACE runs

The meteorological forcing data measured at Champaign, Illinois in 2009 (Ainsworth et al., 2010) were used to drive the JULES-crop model. The downward longwave radiation and diffuse radiation data from NOAA at Bondville site (SURFRAD) were used as SoyFACE does not have these variables available. The driving data were

repeatedly applied (recycled 25 times) to spin up the model from an arbitrary starting point with soil temperature initially set to 278 K and soil moisture to 75% of saturation. A single crop type was modelled – soybean – using a single plant tile. Observed CO_2 (NOAA) and 8-hour mean observed O_3 concentrations from the SoyFACE rings (averaged over a month) were used as the driving data of the model since natural O_3 is produced around 8 hours in daytime and it is a typical temporal resolution for O_3 fumigation. The soil ancillary parameters used in SoyFACE were extracted from the global dataset of soil ancillary from the HadGEM2-ES model (a coupled Earth System Model that was used by the Met Office Hadley Centre for the CMIP5). Observed ambient O_3 were used as the control. The new parameters for soybean were used, which we calibrated to observations from the Mead FLUXNET sites as described in the supplementary material. The exception is the initial carbon: since the row spacing at the SoyFACE experiment is half that used at the Mead sites, we doubled the initial carbon for SoyFACE compared to Mead. The resulting model yield, above ground carbon and LAI was compared to the SoyFACE observations.

3 Results and Discussion

Results from JULES runs with crop model and ozone damage turned on are showed in Figure 3 and 4. Figure 3 shows the evaluation of the soybean aboveground biomass carbon for different O_3 exposure levels (AOT40) using the O_3 damage parameters in Table 4. The model aboveground carbon (solid lines) are compared to the line fitted in Betzelberger et al 2012 to their aboveground carbon observations. The run with the newly-calibrated parameters overestimated the carbon at ambient ozone levels. One contributing factor could be that water stress is underestimated in the new configuration, since it was not possible to evaluate the response to soil water availability using the Mead site data, so we instead derived a value for fsmc_p0 (parameterise in the calculation of the threshold for water stress, see Table 3) from literature. We tested the sensitivity to this choice by re-running this configuration with fsmc_p0=0 which represents water stressed conditions, and this caused a 12% reduction in aboveground carbon (plots show in Supplementary). In addition, the representation of the soil properties in the JULES SoyFACE run could be improved by calibration to site measurements. In contrast, the "Osborne 2015 tuning" intersects the line fitted to observed aboveground carbon at zero ozone concentration (partially because of higher water stress), but then shows a sharp decrease from zero to ambient levels, which is not realistic. Note that no observations were taken for below-ambient ozone concentrations at SoyFACE, so this section of the fitted line is an extrapolation. The slope of the aboveground carbon response to increasing ozone concentrations is similar for all three runs, and compares very well to the Betzelberger et al 2012 fitted line.

270

The yield-O_3 response curve in Figure 4 show that new parametrisation slightly overestimates yield in the ambient SoyFACE ring, compared to the spread of SoyFACE yield observations from Betzelberger et al 2012. The 'Osborne 2015 tuning' with high ozone sensitivity is within the spread of measured yield in ambient conditions, but note that the modelled yield has decreased sharply from zero ozone concentration to ambient levels, which is

275   undesirable. The magnitude of the gradient of yield against AOT40 for all three model configurations is within the spread of the observations. However, the slope is underestimated for the new, calibrated run and overestimated for the 'Osborne 2015 tuning', especially for the range from ambient to 40 ppm h. Recall that ozone concentration modifies net leaf CO_2 assimilation rate in JULES, and that the model parameters governing this process (*Fo3crit, a*) are calibrated directly to net leaf CO_2 assimilation rate observations from SoyFACE in our new configuration

280   (Section 2). Reductions in the modelled net leaf CO_2 assimilation rate lead to the reductions in model aboveground biomass, yield and LAI which we show in this section. However, Betzelberger et al 2012 also reported additional impacts of ozone damage, such as changes in leaf absorptance and specific leaf mass, that are not represented in JULES, and therefore our tuning does not account for them. In contrast, the values of *Fo3crit* and *a* in the high and low sensitivity versions of the 'Osborne 2015 tuning' simulations (table 4) were calibrated in Sitch et al 2007

285   to yield observations. Therefore, they can be seen as 'effective' parameters in these configurations, since they incorporate the effect of the ozone damage processes that are not explicitly represented in JULES.

.

Note that we plot AOT40 on the x-axis for illustrative purposes only, to be comparable with results presented in

290   Betzelberger et al 2012 - AOT40 was not used in the JULES run. An alternative would be to plot ring number or ring target concentration. Ideally, we would plot the x-axis with the metric Phytotoxic Ozone Dose (POD) for JULES and observed data, which account the dosage of O_3 that get into the stomata of soybean, but is beyond the scope of the present study.

295   Figure 5 compares the model and observed LAI at SoyFACE for different O_3 concentrations. JULES was able to reproduce LAI seasonality; however, it underestimated the amplitude. The maximum LAI for calibrated JULES peaked around day 240 in September and observations peaked at DOY 220~230. The peak LAI in the model runs was less than half the observed LAI in all cases. While the Mead model runs also showed a slight underestimation of peak LAI compared to observation (Supplementary Materials), the majority of the underestimation of the

300   modelled SoyFACE LAI is due to a difference between the observed relationships between peak LAI and yield at

the Mead and SoyFACE sites. At both sites, observed maximum yield increases with observed peak LAI. However, for similar observed yields, the observed SoyFACE yield tends to be higher than the observed Mead LAI. Given that our calibration is based on Mead observations, it is therefore not surprising that our model runs at SoyFACE underestimate peak LAI compared to the SoyFACE observations.

305

A contributing factor to the different relationship between observed peak LAI and observed yield at SoyFACE compared to Mead could be the different methods used to measure LAI at the Mead sites (which this parameter set was tuned against) and at SoyFACE. At Mead, destructive measurements were taken, whereas at SoyFACE, LAI was measured indirectly, using radiation attenuation through the canopy.

310

Another plausible contributing factor for the different relationship between observed peak LAI and observed yield at SoyFACE compared to Mead is the row density of the soybean. The SoyFACE row spacing was half that of Mead so, as described above, we set the initial carbon to twice that observed at Mead. The denser planting allowed soybean at SoyFACE to reach higher LAI earlier in the growing season. If this also resulted in thinner leaves at the beginning of the season than with the Mead row spacing, then this could explain the difference in the peak LAI to yield relationship between the two sites. Ricaurte et al., (2016) showed that higher sowing density would increase phyllochron in a linear relationship, which results a higher LAI measured that is consistent with our study. JULES also does not account for leaf age on leaf assimilation rate - in reality a lower leaf assimilation is observed in the late season associated with leaf aging, and it is plausible that this could also be affected by row spacing.

320

Figure 5 also demonstrates that model LAI responds more to ozone concentrations than the observed LAI. One contributing factor is the observed decrease in specific leaf area at SoyFACE in increased ozone (Betzelberger et al 2012). As mentioned above, this process is not captured by JULES. This issue is particularly pronounced in the Osborne 2015 tuning runs, where the modelled LAI in the ring with target 200ppb is roughly a third of the peak LAI in the ambient ring.

325

5 Conclusions

Climate change and air pollution are a great threat to food production. JULES-crop has been developed to represent crops in the land surface model and allow us to estimate the future climate and air pollution impact to crops. The O_3 impact on crops could be quantified with an improved parameterization to the existing O_3 damage

scheme for C3 plants. The default soybean biochemical and respiratory parameters in JULES were based on C3 grass parameters. Characteristics of soybean are more similar to a shrub than grass, therefore parameter calibration is needed to improve the performance of soybean in JULES-crop.

335

In this paper, the parameters needed to describe soybean in JULES-crop were first revised against observations from the Mead FLUXNET sites to ensure that the crop, biochemical and respiratory parameters explicitly represented soybean. Compared with observations from these sites showed that GPP and LAI were well represented for irrigated soybean at Mead. The O_3 damage parameterisation was subsequently calibrated against

340 leaf gas exchange observations from the Soybean Free-Air-Concentration-Enrichment (FACE) experiment for the O_3 damage, by tuning the sensitivity and critical threshold of O_3 damage. On the whole, JULES-Crop reproduces the observed negative correlation between yield and O_3 exposure. It also reproduced the negative impacts of ozone on LAI, and the seasonality of phenology, although the simulated LAI was underestimated at SoyFACE. This method of calibrating soybean could be replicated for other crops once data become available and would contribute

345 to more accurate parameters for crop models. The calibration will be applied to a regional and transient run and eventually the newly calibrated JULES-crop for soybean and its sensitivity to O_3 damage, coupled within an Earth System Model.

350 *Code availability*. This study uses JULES version 5.0 releases. The code and configuration for the SoyFACE runs can be downloaded via the Met Office Science Repository Service (MOSRS) at https://code.metoffice.gov.uk/trac/roses-u/browser/a/r/8/6/6/trunk (JULES Collaboration, 2018)(registration required) and are freely available subject to completion of a software licence. The Leaf Simulator can be downloaded from https://code.metoffice.gov.uk/trac/utils (Williams et al., 2018) (login required).

355

Data availability. Unless otherwise noted, all site observations discussed in this paper were obtained from the Site Information pages of the AmeriFlux website hosted by Oak Ridge National Laboratory

360 (http://fluxnet.fluxdata.org/,(AmeriFlux collaboration, 2018)) or by personal communication with the Mead sites Research Technologist. The longwave radiation, diffuse radiation and air pressure from Bondville, Illinois site is obtained by the SURFRAD (Surface radiation) network from

ftp://aftp.cmdl.noaa.gov/data/radiation/surfrad/Bondville_IL/. The SoyFACE data used for the run are available on MOSRS at:

365 https://code.metoffice.gov.uk/trac/roses-u/browser/a/r/8/6/6/trunk/driving_data
https://code.metoffice.gov.uk/trac/roses-u/browser/a/r/8/6/6/trunk/bin/SoyFACE_gas_exchange_data_2009.csv
https://code.metoffice.gov.uk/trac/roses-u/browser/a/r/8/6/6/trunk/ancil_data
Accessing the MOSRS requires registration, but once you access into the system, there's no information about who is downloading or viewing which pages.

370

Acknowledgements. Felix Leung gratefully acknowledges financial support from the NERC CASE Studentship with Met Office (NE/J017337/1), "Impact of tropospheric O_3 on crop production under future climate and atmospheric CO_2 concentrations, and their interactions within the Earth System". Karina Williams gratefully acknowledges financial support from the European Commission under grant agreements 308291 (EUPORIAS),
375 603864 (HELIX). We acknowledge the following AmeriFlux sites for their data records: US-Ne1, US-Ne1, US-Ne3. In addition, funding for AmeriFlux data resources and core site data was provided by the U.S. Department of Energy's Office of Science. I would also like to acknowledge Gerd Folberth and Eddy Robertson for helping me with the technical part of JULES.

References

380 Agathokleous, E., Vanderstock, A., Kita, K. andKoike, T.: Stem and crown growth of Japanese larch and its hybrid F1 grown in two soils and exposed to two free-air O3 regimes, Environ. Sci. Pollut. Res., 24(7), 6634–6647, doi:10.1007/s11356-017-8401-2, 2017.

Ainsworth, E. a, Yendrek, C. R., Sitch, S., Collins, W. J. andEmberson, L. D.: The effects of tropospheric ozone on net primary productivity and implications for climate change., Annu. Rev. Plant Biol., 63, 637–61,

385 doi:10.1146/annurev-arplant-042110-103829, 2012.

Allen, R. G. andPereira, L. S.: Crop Evapotranspiration (guidelines for computing crop water requirements), Rome. [online] Available from: https://www.kimberly.uidaho.edu/water/fao56/fao56.pdf (Accessed 28September2018), 2006.

AmeriFlux collaboration: AmeriFlux Site Information, [online] Available from: http://fluxnet.fluxdata.org/

390 (Accessed 11November2018), 2018.

Ashmore, M. R.: Assessing the future global impacts of ozone on vegetation, Plant, Cell Environ., 28(8), 949–964, doi:10.1111/j.1365-3040.2005.01341.x, 2005.

Avnery, S., Mauzerall, D. L., Liu, J. andHorowitz, L. W.: Global crop yield reductions due to surface ozone exposure: 1. Year 2000 crop production losses and economic damage, Atmos. Environ., 45(13), 2284–2296,

395 doi:10.1016/j.atmosenv.2010.11.045, 2011a.

Avnery, S., Mauzerall, D. L., Liu, J. andHorowitz, L. W.: Global crop yield reductions due to surface ozone exposure: 2. Year 2030 potential crop production losses and economic damage under two scenarios of O3 pollution, Atmos. Environ., 45(13), 2297–2309, doi:10.1016/j.atmosenv.2011.01.002, 2011b.

Best, M. J., Pryor, M., Clark, D. B., Rooney, G. G., Essery, R. . L. H., Ménard, C. B., Edwards, J. M., Hendry,

400 M. A., Porson, A., Gedney, N., Mercado, L. M., Sitch, S., Blyth, E., Boucher, O., Cox, P. M., Grimmond, C. S. B. andHarding, R. J.: The Joint UK Land Environment Simulator (JULES), model description – Part 1: Energy and water fluxes, Geosci. Model Dev., 4(3), 677–699, doi:10.5194/gmd-4-677-2011, 2011.

Betzelberger, A. M., Yendrek, C. R., Sun, J., Leisner, C. P., Nelson, R. L., Ort, D. R. andAinsworth, E. a: Ozone exposure response for U.S. soybean cultivars: linear reductions in photosynthetic potential, biomass, and yield.,

405 Plant Physiol., 160(4), 1827–39, doi:10.1104/pp.112.205591, 2012.

Büker, P., Morrissey, T., Briolat, a., Falk, R., Simpson, D., Tuovinen, J.-P., Alonso, R., Barth, S., Baumgarten, M., Grulke, N., Karlsson, P. E., King, J., Lagergren, F., Matyssek, R., Nunn, a., Ogaya, R., Peñuelas, J., Rhea, L., Schaub, M., Uddling, J., Werner, W. andEmberson, L. D.: DO3SE modelling of soil moisture to determine ozone flux to forest trees, Atmos. Chem. Phys., 12(12), 5537–5562, doi:10.5194/acp-12-5537-2012, 2012.

410 Clark, D. B., Mercado, L. M., Sitch, S., Jones, C. D., Gedney, N., Best, M. J., Pryor, M., Rooney, G. G., Essery, R. L. H., Blyth, E., Boucher, O., Harding, R. J., Huntingford, C. andCox, P. M.: The Joint UK Land Environment Simulator (JULES), model description – Part 2: Carbon fluxes and vegetation dynamics, Geosci. Model Dev., 4(3), 701–722, doi:10.5194/gmd-4-701-2011, 2011.

Dentener, F., Keating, T., and Akimoto, H.: Hemispheric Transport of 2010 Part a : Ozone and Particulate

415 Matter, Air Pollut. Stud., (17), 278 [online] Available from: https://www.unece.org/fileadmin/DAM/env/lrtap/Publications/11-22136-Part-D_01.pdf (Accessed 18March2013), 2010.

Dermody, O., Long, S. P., McCONNAUGHAY, K. andDeLUCIA, E. H.: How do elevated CO 2 and O 3 affect

the interception and utilization of radiation by a soybean canopy?, Glob. Chang. Biol., 14(3), 556–564,

420   doi:10.1111/j.1365-2486.2007.01502.x, 2008.

VanDingenen, R., Dentener, F. J., Raes, F., Krol, M. C., Emberson, L. andCofala, J.: The global impact of

ozone on agricultural crop yields under current and future air quality legislation, Atmos. Environ., 43(3), 604–

618, doi:10.1016/j.atmosenv.2008.10.033, 2009.

Elagöz, V. andManning, W. J.: Responses of sensitive and tolerant bush beans (Phaseolus vulgaris L.) to ozone

425   in open-top chambers are influenced by phenotypic differences, morphological characteristics, and the chamber

environment, Environ. Pollut., 136(3), 371–383, doi:10.1016/j.envpol.2005.01.021, 2005.

Emberson, L. D., Büker, P. andAshmore, M. R.: Assessing the risk caused by ground level ozone to European

forest trees: A case study in pine, beech and oak across different climate regions, Environ. Pollut., 147(3), 454–

466, doi:10.1016/j.envpol.2006.10.026, 2007.

430   Fuhrer, J.: Ozone risk for crops and pastures in present and future climates., Naturwissenschaften, 96(2), 173–

94, doi:10.1007/s00114-008-0468-7, 2009.

Fuhrer, J., Skärby, L. andAshmore, M. R.: Critical levels for ozone effects on vegetation in Europe., Environ.

Pollut., 97(1–2), 91–106 [online] Available from: http://www.ncbi.nlm.nih.gov/pubmed/15093382, 1997.

Gerosa, G., Finco, a., Marzuoli, R., Ferretti, M. andGottardini, E.: Errors in ozone risk assessment using

435   standard conditions for converting ozone concentrations obtained by passive samplers in mountain regions, J.

Environ. Monit., 14(6), 1703, doi:10.1039/c2em10965d, 2012.

Gleckler, P. J., Taylor, K. E. andDoutriaux, C.: Performance metrics for climate models, J. Geophys. Res.,

113(D6), D06104, doi:10.1029/2007JD008972, 2008.

Van denHoof, C., Hanert, E. andVidale, P. L.: Simulating dynamic crop growth with an adapted land surface

440   model – JULES-SUCROS: Model development and validation, Agric. For. Meteorol., 151(2), 137–153,

doi:10.1016/j.agrformet.2010.09.011, 2011.

ICP Vegetation: Mapping Critical Levels for Vegetation, Chapter III. Manual on Methodologies and Criteria for

Modelling and Mapping Critical Loads and Levels and Air Pollution Effects, Risks and Trends., Conv. Long-

range Transbound. Air Pollut., 2017(April), 1–66 [online] Available from:

445   https://www.umweltbundesamt.de/sites/default/files/medien/4292/dokumente/ch3-mapman-2017-10.pdf, 2017.

JULES Collaboration: ULES collaboration: JULES land-surface model, [online] Available from:

https://code.metoffice.gov.uk/trac/jules/ (Accessed 11November2019), 2018.

Knutti, R., Masson, D. andGettelman, A.: Climate model genealogy: Generation CMIP5 and how we got there,

Geophys. Res. Lett., 40(6), 1194–1199, doi:10.1002/grl.50256, 2013.

450   Leung, F., Pang, J. Y. S., Tai, A. P. K., Lam, T., Tao, D. K. C. andSharps, K.: Evidence of Ozone-Induced

Visible Foliar Injury in Hong Kong Using Phaseolus Vulgaris as a Bioindicator, Atmosphere (Basel)., 11(3),

266, doi:10.3390/atmos11030266, 2020.

Long, S. P., Ainsworth, E. a, Leakey, A. D. B. andMorgan, P. B.: Global food insecurity. treatment of major

food crops with elevated carbon dioxide or ozone under large-scale fully open-air conditions suggests recent

455   models may have overestimated future yields., Philos. Trans. R. Soc. Lond. B. Biol. Sci., 360(1463), 2011–20,

doi:10.1098/rstb.2005.1749, 2005.

Mills, G., Buse, A., Gimeno, B., Bermejo, V., Holland, M., Emberson, L. andPleijel, H.: A synthesis of AOT40-

based response functions and critical levels of ozone for agricultural and horticultural crops, Atmos. Environ.,

41(12), 2630–2643, doi:10.1016/j.atmosenv.2006.11.016, 2007.

460   Morgan, P. B., Ainsworth, E. a. andLong, S. P.: How does elevated ozone impact soybean? A meta-analysis of photosynthesis, growth and yield, Plant, Cell Environ., 26(8), 1317–1328, doi:10.1046/j.0016-8025.2003.01056.x, 2003.

Oliver, R. J., Mercado, L. M., Sitch, S., Simpson, D., Medlyn, B. E., Lin, Y.-S., Folberth, G. A. andOliver, R. J.: Large but decreasing effect of ozone on the European carbon sink, Biogeosciences, 15, 4245–4269,

465   doi:10.5194/bg-15-4245-2018, 2018.

Osborne, T. andHooker, J.: JULES-crop technical documentation Crop parameterisation, Univ. Read., 1–49, 2011.

Osborne, T., Gornall, J., Hooker, J., Williams, K., Wiltshire, A., Betts, R. andWheeler, T.: JULES-crop: a parametrisation of crops in the Joint UK Land Environment Simulator, Geosci. Model Dev, 8, 1139–1155,

470   doi:10.5194/gmd-8-1139-2015, 2015.

Paoletti, E., Materassi, A., Fasano, G., Hoshika, Y., Carriero, G., Silaghi, D. andBadea, O.: A new-generation 3D ozone FACE (Free Air Controlled Exposure), Sci. Total Environ., 575, 1407–1414, doi:10.1016/j.scitotenv.2016.09.217, 2017.

Pleijel, H., Danielsson, H., Emberson, L., Ashmore, M. R. andMills, G.: Ozone risk assessment for agricultural

475   crops in Europe: Further development of stomatal flux and flux–response relationships for European wheat and potato, Atmos. Environ., 41(14), 3022–3040, doi:10.1016/j.atmosenv.2006.12.002, 2007.

Ray, D. K., Mueller, N. D., West, P. C., Foley, J. A., Pingali, P., Godfray, H., Beddington, J., Crute, I., Haddad, L., Lawrence, D., Tilman, D., Balzer, C., Hill, J., Befort, B., Foley, J., Ramankutty, N., Brauman, K., Cassidy, E., Gerber, J., Phalan, B., Balmford, A., Green, R., Scharlemann, J., Phalan, B., Onia, M., Balmford, A., Green,

480   R., Green, R., Cornell, S., Scharlemann, J., Balmford, A., Matson, P., Vitousek, P., Tscharntke, T., Clough, Y., Wanger, T., Jackson, L., Motzke, I., Hulme, M., Vickery, J., Green, R., Phalan, B., Chamberlain, D., Andrew, D., Ephraim, C., Pingali, P., Cassman, K., Finger, R., Peltonen-Sainio, P., Jauhiainen, L., Laurila, I., Brisson, N., Gate, P., Gouache, D., Charmet, G., Francois-Xavier, O., Lin, M., Huybers, P., Ray, D., Ramankutty, N., Mueller, N., West, P., Foley, J., Hafner, S., Dyson, T., Dawe, D., Dobermann, A., Moya, P., Abdulrachman, S.,

485   Singh, B., Ladha, J., Dawe, D., Pathak, H., Padre, A., Yadav, R., Fischer, R., Edmeades, G., Jaggard, K., Qi, A., Ober, E., Supit, I., Foley, J., DeFries, R., Asner, G., Barford, C., Bonan, G., Rockström, J., Steffen, W., Noone, K., Persson, A., Chapin, S., Donald, P., Green, R., Heath, M., Heathcote, A., Filstrup, C., Downing, J., Eickhout, B., Bouwman, A., et al.: Yield Trends Are Insufficient to Double Global Crop Production by 2050, edited by J. P.Hart, PLoS One, 8(6), e66428, doi:10.1371/journal.pone.0066428, 2013.

490   Sitch, S.: Carbon sinks threatened by increasing ozone, Nat. Publ. Gr., 7(8), 2335–40, doi:10.1021/nl0709975, 2007.

Sitch, S., Cox, P. M., Collins, W. J. andHuntingford, C.: Indirect radiative forcing of climate change through ozone effects on the land-carbon sink., Nature, 448(7155), 791–4, doi:10.1038/nature06059, 2007.

Tai, A. P. K. andVal Martin, M.: Impacts of ozone air pollution and temperature extremes on crop yields:

495   Spatial variability, adaptation and implications for future food security, Atmos. Environ., 169, 11–21, doi:10.1016/J.ATMOSENV.2017.09.002, 2017.

Tai, A. P. K., Martin, M. V. andHeald, C. L.: Threat to future global food security from climate change and ozone air pollution, Nat. Clim. Chang., 4(9), 817–821, doi:10.1038/NCLIMATE2317, 2014.

Williams, K., Gornall, J., Harper, A., Wiltshire, A., Hemming, D., Quaife, T., Arkebauer, T. andScoby, D.:
500 Evaluation of JULES-crop performance against site observations of irrigated maize from Mead, Nebraska,
Geosci. Model Dev, 10(3), 1291–1320, doi:10.5194/gmd-10-1291-2017, 2017.

Williams, K., Hemming, D., Harper, A. B. andMercado, L. M.: Leaf simulator, 2018.

505
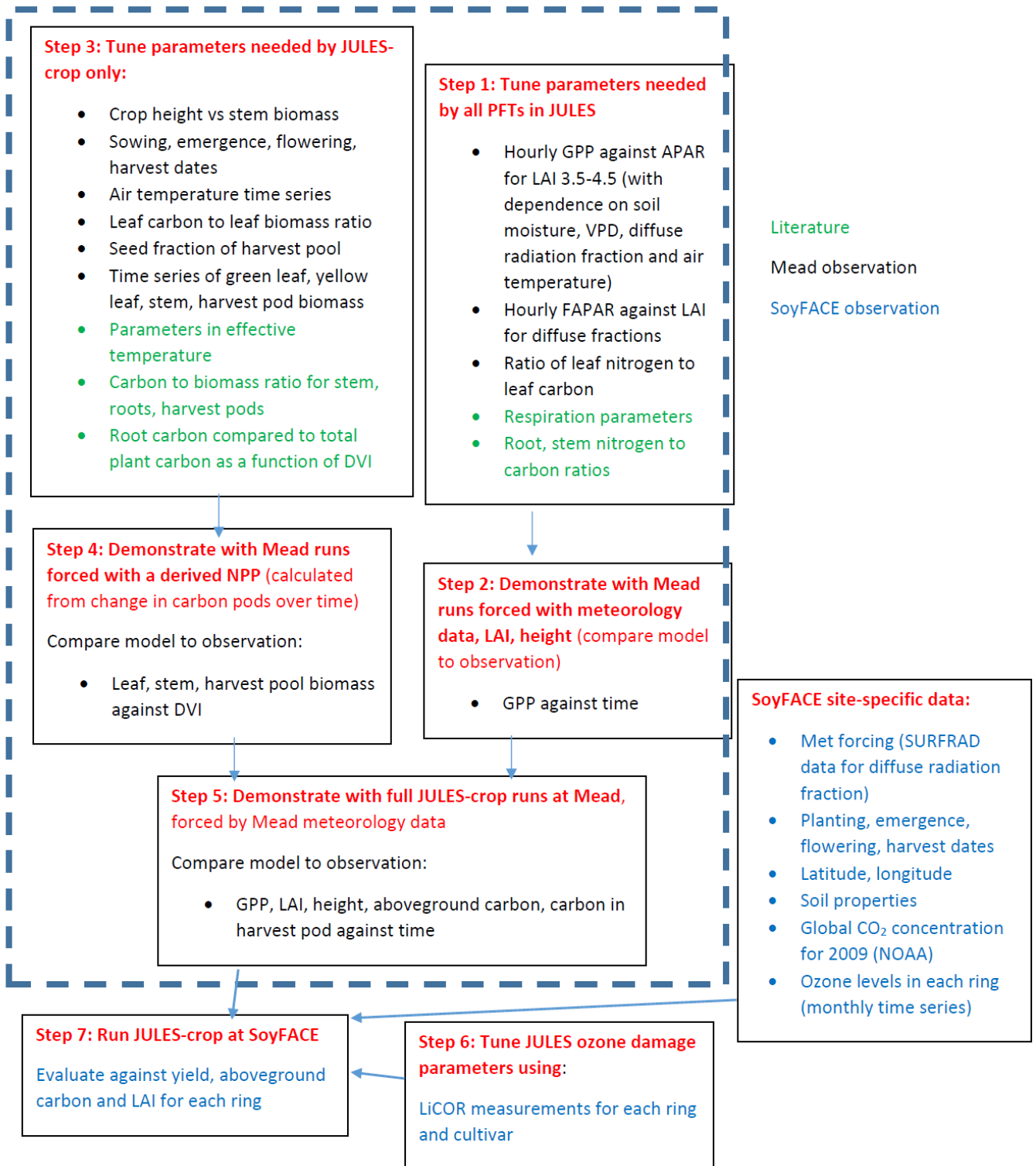
510   Figure 1. Flowchart of tuning the parameters and calibrating the model
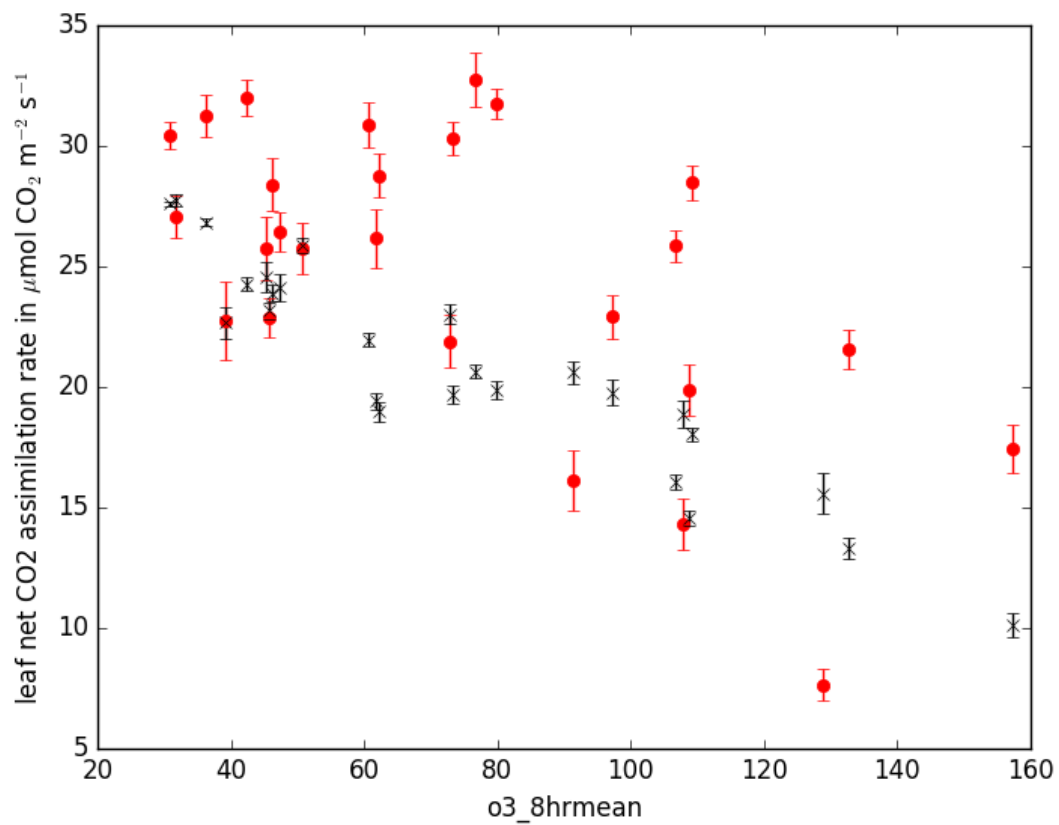
Figure 2. Net leaf CO$_2$ assimilation rate for calibrated JULES, simulated using the Leaf Simulator (black crosses) and observations from Betzelberger et al., (2012) (grey circles). X-axis is the daytime 8-hour mean O$_3$
515   concentration (ppb) .
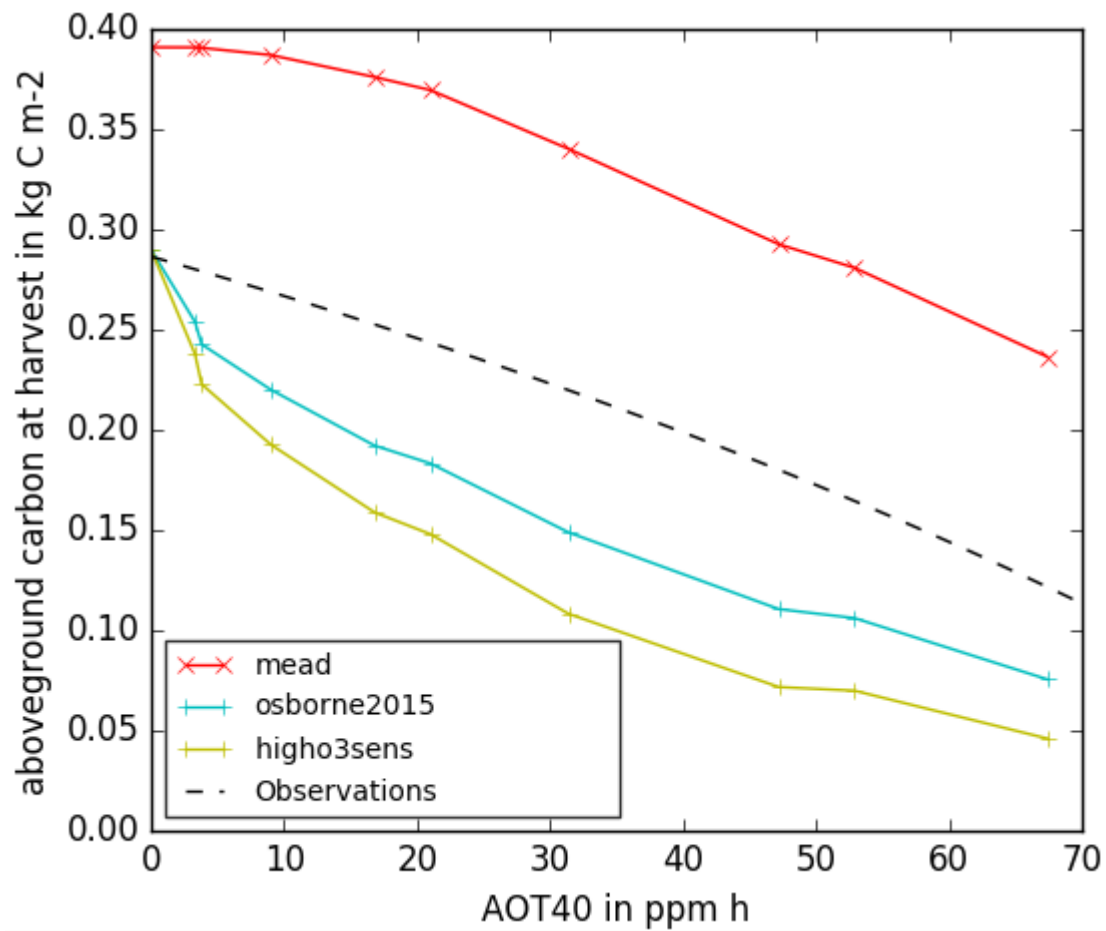
Figure 3. Aboveground carbon biomass of soybean at harvest stage for calibrated Joint UK Land Environment Simulator with Crop module turned on (JULES-crop) using the Mead soybean tuning (red), Osborne et al. (2015) standard parameters with Sitch et al. (2007) low ozone sensitivity (blue), high ozone sensitivity (green) and observation from SoyFACE from Betzelberger et al. 2012.
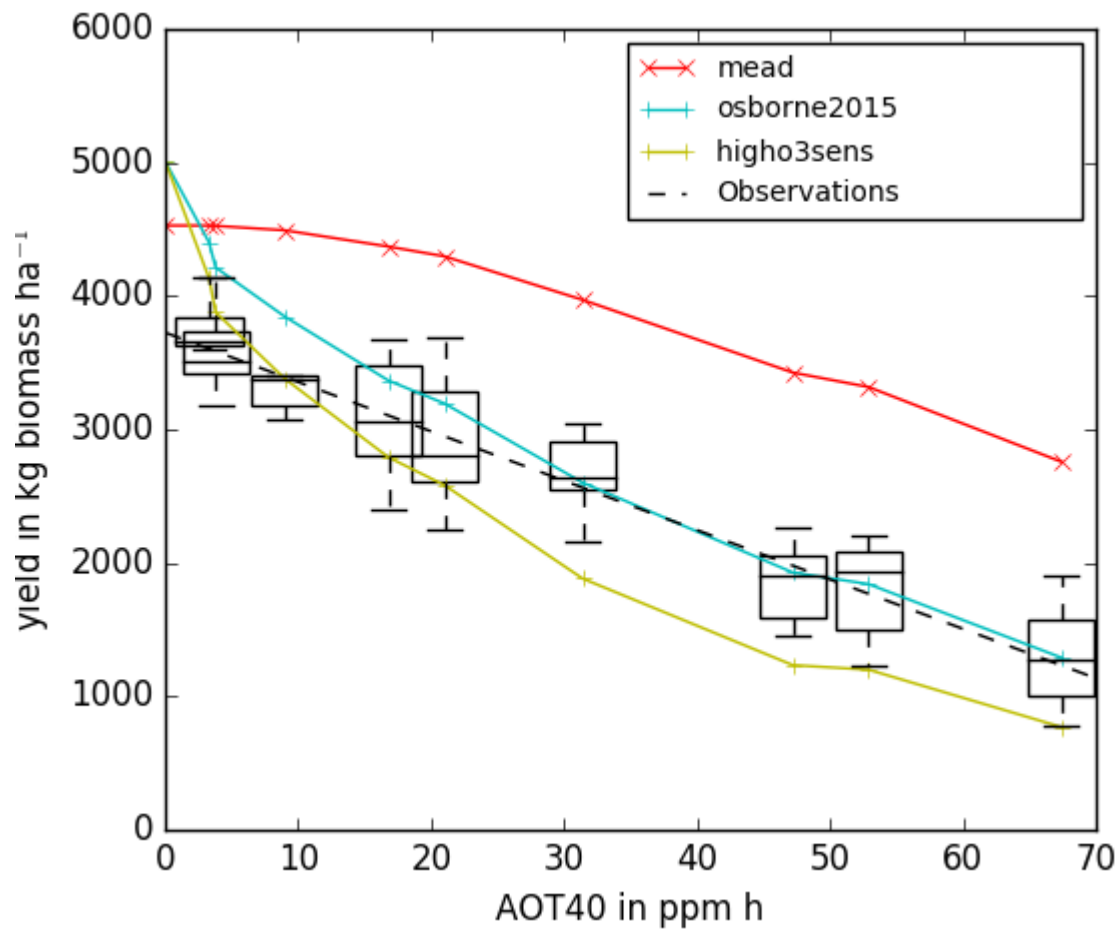
Figure 4 Black dashed line is the line of best fit from SoyFACE observation and the blue and green lines with crosses are the modelled output for each ozone concentration using the Osborne et al 2015 tuning with Sitch et al 2007 low and high sensitivity, respectively. The red line and crosses are the tuned parameters with Mead FLUXNET observation and SoyFACE ozone damage according to Table 4.
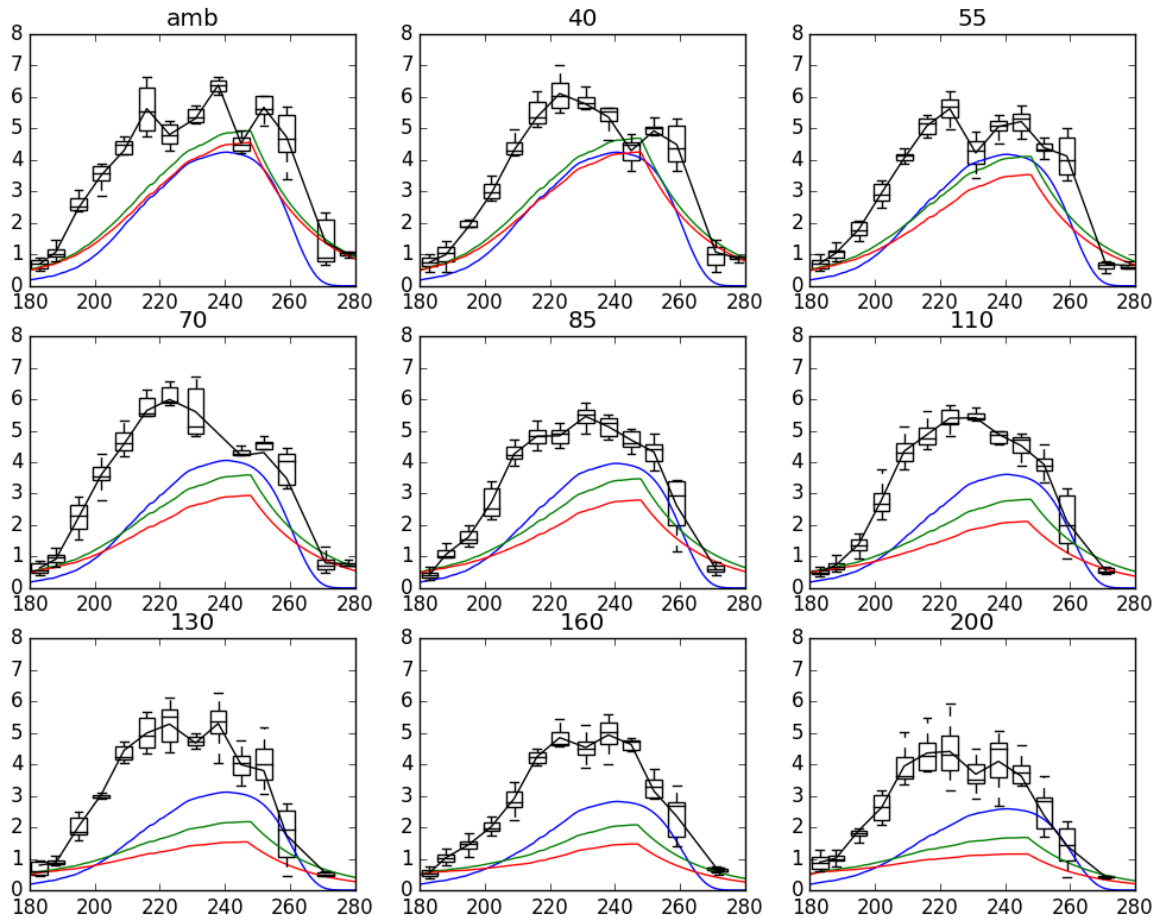
Figure 5 Time series of Leaf Area Index (LAI) responses on different target ozone concentration at SoyFACE.
Black line is observed LAI from Betzelberger et al., (2012) and the other lines are JULES-crop LAI with
different tunings. Blue: calibrated JULES-crop using Mead observations. Green: Osborne 2015 tuning with low
sensitivity. Red: Osborne 2015 tuning with high sensitivity to ozone.

Table 1. JULES modules switches, which F (False) means turned off and T (True) means turned on. Asterisk indicates parameter was hard-wired and the description of the parameters at the bottom

	Osborne et al., (2015)	This study	Discussion
can_rad_mod	5 (6 was not available)	6	Recommended option for layered canopy in version 4.6
l_irrig_dmd	F	T	Irrigation on
irr_crop	-	0	
l_trait_phys	F	F	
l_scale_resp_pm	F	T	
l_leaf_n_resp_fix	F	-	Bug fix, affects can_rad_mod=5 but not can_rad_mod=6
l_prescsow	T	T	Sowing dates available

Parameters	Description
Canopy radiation model	Number 6 is Multi-layer approach for radiation interception following the 2-stream approach of Sellers et al. (1992). This approach takes into account leaf angle distribution, zenith angle, and differentiates absorption of direct and diffuse radiation. it has a decline of leaf N with canopy height. Additionally includes inhibition of leaf respiration in the light. including: Sunfleck penetration though the canopy. Division of sunlit and shaded leaves within each canopy level. A modified version of inhibition of leaf respiration in the light. exponential decline of leaf N with canopy height proportional to LAI, following Beer's law.
L_irrid_dmd	Switch controlling the implementation of irrigation demand code.
Irr_crop	Irrigation season (i.e. season in which crops might be growing on the gridbox) lasts the entire year.
l_trait_phys	Switch for using trait-based physiology. Vcmax is calculated based on parameters nl0 (kgN kgC-1) and neff.
l_scale_resp_pm	Soil moisture stress reduces leaf, root, and stem maintenance respiration.
l_leaf_n_resp_fix	Switch for bug fix for leaf nitrogen content used in the calculation of plant maintenance respiration.
l_prescsow	Sowing dates prescribed

Table 2. Parameter values in JULES-crop that are used to represent soybean. Asterisk indicates parameter was hard-wired.

		Osborne et al., (2015)	This study	Discussion
T_b	Base temperature (K)	278.15	278.15	Kept at Osborne et al., (2015) value
T_o	Optimum temperature(K)	313.15	313.15	Kept at Osborne et al., (2015) value
T_m	Maximum temp (K)	300.15	300.15	Kept at Osborne et al., (2015) value
P_{sen}	Sensitivity of development rate to photoperiod (hours-1)	0.0	0.0	Kept at Osborne et al., (2015) value
P_{crit}	Critical photoperiod (hours)	-	-	Not used when $P_{sen} = 0$
r_{dir}	coefficient determining relative growth of roots vertically and horizontally	0.0	0.0	Kept at Osborne et al., (2015) value
α_{root}	coefficient of partitioning to root	20.0	19.8	Supplementary Material 1.4.1
α_{stem}	coefficient of partitioning to stem	18.5	18.5	Supplementary Material 1.4.1
α_{leaf}	coefficient of partitioning to leaf	19.5	19.2	Supplementary Material 1.4.1
β_{root}	coefficient of partitioning to root	-16.5	-15.47	Supplementary Material 1.4.1
β_{stem}	coefficient of partitioning to stem	-14.5	-13.195	Supplementary Material 1.4.1
β_{leaf}	coefficient of partitioning to leaf	-15.0	-14.287	Supplementary Material 1.4.1
γ	coefficient of specific leaf area ($m^2\ kg^{-1}$)	25.9	24.0	Supplementary Material 1.4.3
δ	coefficient of specific leaf area ($m^2\ kg^{-1}$)	-0.1451	0.15	Supplementary Material 1.4.3
τ	Remobilisation factor, fraction of stem growth partitioned to RESERVEC	0.18	0.26	Supplementary Material 1.4.3
$f_{C,root}$	Carbon fraction for dry root	0.5	0.47	Supplementary Material 1.4.4
$f_{C,stem}$	Carbon fraction for dry stem	0.5	0.49	Supplementary Material 1.4.4
$f_{C,leaf}$	Carbon fraction for dry leaf	0.5	0.46	Supplementary Material 1.4.4

$f_{C,harv}$	Carbon fraction for harvest	0.5	0.53	Supplementary Material 1.4.4
κ	Allometric coefficient relating STEMC to CANHT	1.6	1.9	Supplementary Material 1.4.2
λ	Allometric coefficient relating STEMC to CANHT	0.4	0.47	Supplementary Material 1.4.2
μ	Allometric coefficient for calculation of senescence	0.05*	5.0	Supplementary Material 1.4.2
v	Allometric coefficient for calculation of senescence	0.0*	6.0	Supplementary Material 1.4.2
DVI_{sen}	DVI at which leaf senescence begins	1.5*	1.25	Supplementary Material 1.5
C_{init}	Carbon in crop at emergence in kgC/m2.	0.01*	3.5E-3 (Mead), 7.0E-3(SoyFACE)	Supplementary Material 1.4.5
DVI_{init}	DVI at which the crop carbon is set to initial carbon	0.0*	0.2	Supplementary Material 1.4.5
T_{mort}	Soil temperature (second level) at which to kill crop if DVI>1	t_bse_io*	263.15	Section 2.3
f_{yield}	Fraction of the harvest carbon pool converted to yield carbon	1.0*	0.74	Section 2.3

565

570

575

Table 3. JULES plant functional type parameters extended to represent soybean. Asterisk indicates parameter was hard-wired.

		Osborne et al., (2015)	This study	Discussion
$c3$	c3_io	1	1	Soybean is a C3 plant.
dr	rootd_ft_io	0.5	0.5	Not important in irrigated runs, so could not be tuned using US-Ne2 data. Kept at Osborne et al, (2015) value
$dq\text{crit}$	dq_crit_io	0.1	0.1	Kept at Osborne et al., (2015) value
f_d	fd_io	0.015	0.008	Supplementary Material 1.4.6
$f0$	f0_io	0.9	0.9	Kept at Osborne et al., (2015) value
$n\text{eff}$	neff_io	8.0×10^{-4}	12.0×10^{-4}	Table 1
$n_l(0)$	nl0_io	0.073	0.1	Table 1
$T\text{low}$	tlow_io	0.0	0.0	Kept at Osborne et al., (2015) value
$T\text{upp}$	tupp_io	36.0	36.0	Kept at Osborne et al., (2015) value
k_n	kn_io	0.78	-	Default for C3 grass for can_rad_mod5.
k_{nl}	knl_io	-	0.2	Default for C3 grass for can_rad_mod6.
$Q10,\text{leaf}$	q10_leaf_io	2.0	2.0	Kept at Osborne et al., (2015) value
μ_{rl}	nr_nl_io	1.0	0.390	Supplementary Material S1-3
μ_{sl}	ns_nl_io	1.0	0.51	Supplementary Material S1-3
r_g	r_grow_io	0.25	0.32	Supplementary Material 1.4.6
	orient_io	0	0	Kept at Osborne et al., (2015) value
α	alpha_io	0.12	0.12	Kept at Osborne et al., (2015) value
ωPAR	omega_io	0.15	0.15	Kept at Osborne et al., (2015) value
αPAR	alpar_io	0.1	0.1	Kept at Osborne et al., (2015) value
	fsmc_mod_io	0	0	Not important in irrigated runs, so could not be tuned using US-Ne2 data. Kept at Osborne et al (2015) value.
	fsmc_p0_io	0.0	0.5	FAO document 56 (Allen andPereira, 2006)
a	can_struct_a_io	1.0	1.0	Kept at Osborne et al., (2015) value

Table 4. Summary of ozone parameter configurations employed in JULES-crop for the default Osborne et al., (2015) value and the tuned as calibrated to SoyFACE leaf gas-exchange measurements (note that these have been calibrated to daytime 8-hour concentrations and therefore will be different to parameters calibrated to monthly 24hour means)

JULES ozone damage Parameters	Fractional reduction of photosynthesis by O_3 (sensitivity) ($mmol^{-1}$ m^2) (dfp_dcuo_io)	Threshold of ozone flux ($nmol$ m^{-2} s^{-1}) (fl_o3_ct_io)
Tuned value	0.5	15.0
Osborne et al 2015 (High sensitivity)	5.0	1.4
Osborne et al 2015 (Low sensitivity)	5.0	0.25

590

595